PSIM simulation and analysis of LCC series-parallel resonant converter

Harun Özbay[1]
[1]*Bandırma Onyedi Eylül University, Dept. of Electrical Engineering, Bandırma, Balıkesir, Turkey, hozbay@bandirma.edu.tr, ORCID: 0000-0003-1068-244X*

In the control of DC-DC converters, pulse width modulation (PWM) is commonly used. In converters operating with PWM control, the switches operate under hard-switching conditions, resulting in increased switching losses, current and voltage stresses on the switching elements, and electromagnetic interference (EMI) noise as the operating frequency increases. Achieving higher power density and faster transient response in DC-DC converters is possible only by increasing the switching frequency. Therefore, reducing these losses and noises while increasing the switching frequency is only possible with soft switching techniques. Particularly in cases of variable loads, such as batteries, and when a smoother output voltage is required, the series-parallel LCC-type circuit topology from resonant converter topologies is employed. In this study, a simple algorithm has been developed to rapidly control the output voltage and switching frequency of the Full-Bridge Isolated LCC Series-Parallel Resonance circuit based on the current drawn by the changing load over time. The circuit has been successfully operated in the range of 100-130 kHz.

Keywords: *Resonant converter, LCC, Zero current switching, PSIM.*

1. Introduction

Pulse Width Modulation (PWM) converters enable the flow of power between the power source and the load through the abrupt switching of semiconductor switches. Semiconductors operate in switching mode, and the transition from on to off state of the switch occurs under full load current. During opening and closing, switches are exposed to significant opening-closing voltages. At the same time, in switches, there is a power loss that linearly increases with the switching frequency. Another drawback of operating in the switching mode is the occurrence of high electromagnetic interference (EMI) due to the large di/dt and dv/dt during switching. The foundation of soft switching technique relies on bringing the switches to the on or off state when the current, voltage, or both are at zero values on semiconductor circuit elements [1-4].

To reduce the volume and weight of power electronic converters and increase power density, it is necessary to increase the switching frequency. In this case, the problems arising from operating in the switching mode become more significant. However, these issues can be minimized by making the switch voltage or current zero at the moment of switching from on to off or vice versa. This process is referred to as zero voltage or zero current switching. Many of these circuit structures operate according to the L-C resonance phenomenon, and therefore, these circuits are generally referred to as "resonant converters" [5-7].

Reducing the switching voltages in converters operating in the switching mode is achieved by using snubber circuits consisting of diodes connected in series and parallel with the switch, along with passive damping elements. However, in such circuits, the switching losses occurring in the switch are transferred to the snubber circuit, and therefore, no increase in overall efficiency can be achieved. In converters operating in the switching mode, if one of the switch current or switch voltage can be made zero during switching, in the opposite direction of the function provided by the snubber circuits, the switching stresses, switching losses, and EMI problems arising from switching can be overcome. Ideally, during the switching transition event, both voltage and current should be zero [7-10].

Soft switching topologies are created by adding a high-frequency resonant arm to the traditional hard-switching topology. As a result, the switch current or voltage oscillates at the zero point, creating soft switching conditions for power elements. Switching waveforms can be shaped by the resonant arm to trim switching losses and stresses, thus reducing EMI. The selection of the resonant arm scheme depends on the current and voltage waveforms that will occur in the converter. This implies that there can be various ways of classifying topologies [11-14].

The structure of the Series-Parallel Resonant converter incorporates advantageous aspects of both series resonant and parallel resonant converters. The circuit topology is formed by connecting a half-bridge or full-bridge series-parallel inverter and a voltage-controlled rectifier in series. The load is connected in parallel with a resonant capacitor in the series-parallel inverter. If the reactance of this capacitor is smaller than the input impedance of the rectifier, the output voltage of the inverter becomes close to sinusoidal, and the inverter behaves like a sine wave voltage source. In this case, the series-parallel resonant inverter operates compatibly with voltage-controlled rectifiers. If these conditions are not satisfactorily met, the output voltage of the inverter is formed in a non-sinusoidal form [15].

2. Series-Parallel resonant circuit (LCC) topology

Figure 1 shows the series-parallel LCC resonance circuit topology, including three different rectifier types. The inverter section consists of two bidirectional switches, S1 and S2, and resonant circuit elements L, C1, and C2. Similar to the series resonant converter, the C1 capacitor and L coil are connected in series. The C2 capacitor is connected in parallel, similar to the parallel resonant converter. As the MOSFET switches have their own body diode, they can conduct current in both directions. The switching elements perform switching at the switching frequency ($f=\omega/2\pi$) with a duty cycle of 50%, acting as a square-wave voltage source. If the C1 capacitor is chosen to be excessively large, the circuit behaves like a parallel resonant converter. On the other hand, if the C2 capacitor is excessively small, the circuit behaves like a series resonant converter. In fact, transformer series resonant circuits behave like a series-parallel resonant circuit due to the stray inductance of the transformer. For these reasons, the series-parallel resonance topology operates between the characteristics of series and parallel resonance circuit topologies [1].

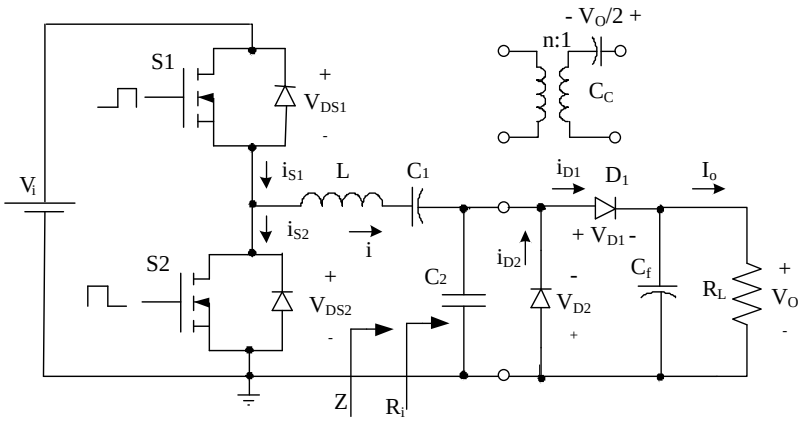

***Figure 1**. Series-Parallel resonant converter.*

The output voltage of the inverter is rectified using any rectifier shown in Figure 1. Since the output voltage is highly sensitive to the switching frequency, the output voltage is controlled by varying the frequency over wide ranges. The C2 capacitor can also be placed on the other side of the transformer. In this case, the capacitance of the transformer windings is absorbed by the C2 capacitor, and the leakage magnetic inductance of the transformer is absorbed by the L inductor. Therefore, if there are parasitic transformer components in the circuit, this circuit topology is preferred.
Instead of rectifiers, a square wave current source can be connected, as seen in Figure 2a. The switches can be replaced with internal resistances Ri, as shown in Figure 2b. The parallel Ri-C circuit in Figure 2b is converted to the series Rs-Cs circuit in Figure 2c. In Figure 2d, a DC voltage source Vi and switches S1, S2 are replaced with a 0-Vi square wave voltage source. In this case, the total parasitic resistance is r=rDS+rL, and the total resistance of the circuit is R=Rs+r.

If the switching frequency is greater than the resonant frequency ($f > fr = 1/\sqrt{(LCeq)}$), the current and voltage waveforms resemble those of a parallel resonant converter. It should be noted that Ceq=C1Cs/(C1+Cs) in this case. If the quality factor is large, the current flowing through the L coil will be close to sinusoidal, and the converter will operate in continuous conduction mode. The first half-period of this current flows through switch S1 when it is open, and the second half-period flows through switch S2 when it is open. Selecting the operating frequency above the resonant frequency is not harmful for the parallel diodes on the MOSFETs when recovering in the reverse direction [2].

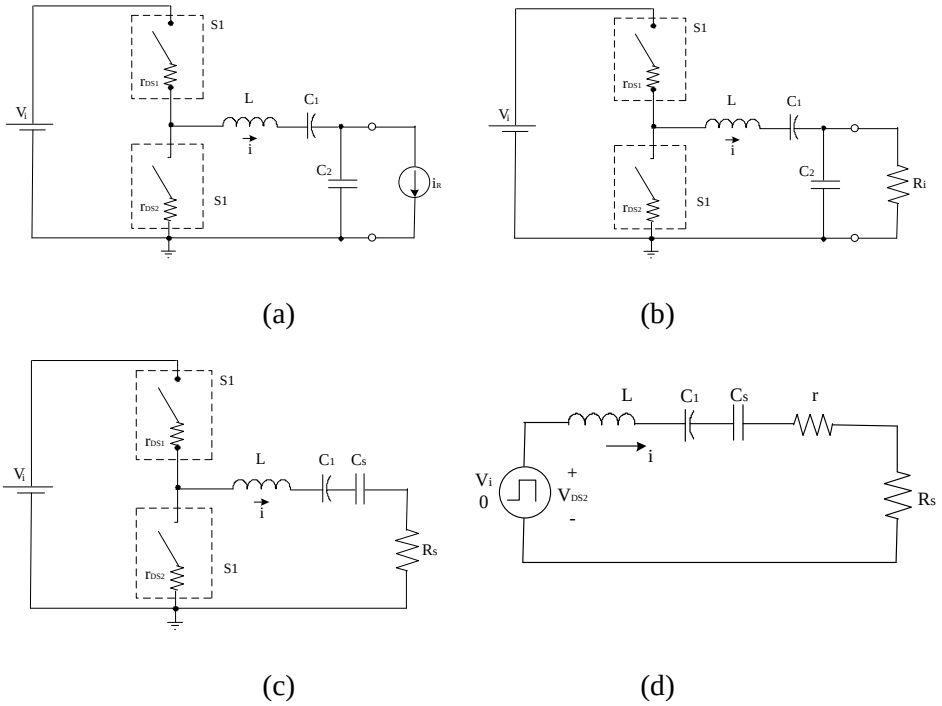

Figure 2*. Converter equivalent circuit (a) A square wave current source is connected instead of a rectifier (b) An internal resistance is connected instead of a rectifier (c) The parallel circuit is converted into a series Cs-Rs circuit (d) The switching elements are removed and a square wave voltage source is connected.*

3. Circuit analysis of series parallel resonant converter

In series resonant converters, the maximum value of the current flowing through the resonant circuit is inversely proportional to the load. Thus, at low loads, conduction losses decrease, leading to an increase in partial load efficiency. In parallel resonant converters, however, the maximum value of the current flowing through the resonant coil is entirely dependent on the load resistance. This is because most of the current flowing through the resonant coil connected in parallel to the resonant capacitor passes through the load resistance. Consequently, due to constant conduction losses, the partial load efficiency will be weak. In the series-parallel resonant converter, if Ri << XC2 = 1/ωC2, most of the current through the coil passes through the load resistance. However, the maximum value of the current flowing through the resonant circuit is inversely proportional to the load. Thus, with the series-parallel resonant converter, more efficient output power can be obtained at higher powers without constant losses [1]. The analysis of the circuit in Figure 1 in the time domain is as follows:

$$R_{i\min} = \frac{\pi^2}{2} R_{L\min} \left(1 + \frac{V_F}{V_O} + \frac{R_F + r_{LF}}{R_{L\min}} \right) \tag{1}$$

$$R_{L\min} = \frac{V_o^2}{P_{o\max}} \tag{2}$$

$$M_{VR} = \frac{\sqrt{2}}{\pi \left(1 + \frac{V_F}{V_O} + \frac{R_F + r_{LF}}{R_{L\min}} \right)} \tag{3}$$

$$M_V = \frac{V_O}{V_i} \tag{4}$$

$$Q_L = \frac{\frac{\omega}{\omega_0}}{\sqrt{\frac{1}{M_{Vr}{}^2} - \left[1 - \left(\frac{\omega}{\omega_0}\right)^2\right]^2}} \tag{5}$$

$$L = \frac{R_{i\min}}{\omega_0 Q_L} \tag{6}$$

$$C = \frac{Q_L}{\omega_0 R_i} \tag{7}$$

$$A = \frac{C_2}{C_1} \tag{8}$$

$$C_1 = C\left(1 + \frac{1}{A}\right),\ C_2 = C\left(1 + \frac{1}{A}\right) \tag{9}$$

$$Z_o = \sqrt{\frac{L}{C_{eq}}} \tag{10}$$

$$I_{SM_{\max}} = \mathrm{I_m} = \frac{2V_i}{\pi R_{i\min}} \sqrt{\frac{1 + \left[Q_L\left(\frac{\omega}{\omega_o}\right)(1+A)\right]^2}{(1+A)^2\left[1 - \left(\frac{\omega}{\omega_o}\right)^2\right]^2 + \frac{1}{Q_L^2}\left(\frac{\omega}{\omega_o} - \frac{\omega_o}{\omega}\frac{A}{A+1}\right)^2}} \tag{11}$$

$$\eta = \eta_I . \eta_R \tag{12}$$

$$P_{\mathrm{Im}ax} = \frac{P_{0\max}}{\eta} \tag{13}$$

4. PSIM simulation study of full bridge LCC circuit

In this study, a simple algorithm has been developed to rapidly control the output voltage and switching frequency of the Full-Bridge Isolated LCC Series-Parallel Resonance circuit based on the current drawn by the changing load over time. The circuit is designed to operate with an input voltage of 550V, an output voltage of 400V, a maximum output current of 25A, and a variable operating frequency between 100-130kHz depending on the load condition. The algorithm detects the current flowing through the resonance circuit and the output voltage through sensors, ensuring the continuous resonance operation of the system and maintaining the output voltage at 400 volts even when the load changes. The S1 and S3 switches in the circuit perform switching in zero current and zero voltage conditions. The S2 and S4 switches, on the other hand, perform zero voltage switching by phase shifting according to the power state. The drawings and simulation results of the circuit using the PSIM program are presented in Figures 3.

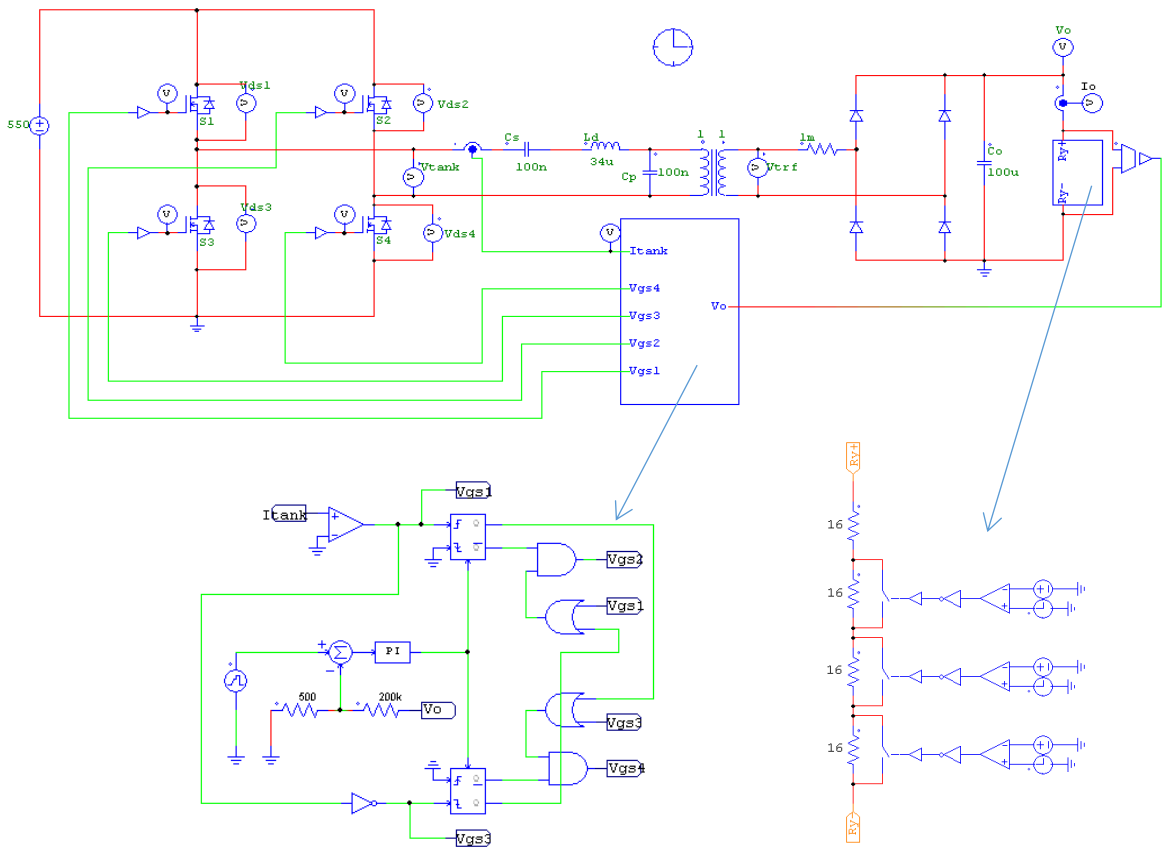

***Figure 3**. Simulation of LCC resonant converter at different loads.*

The developed algorithm detects the current flowing through the resonance circuit and the output voltage, ensuring continuous resonance operation of the system and maintaining the output voltage at 400 volts even during load changes. Figure 4 shows the variation in output voltage and output current over time. When the system is started, it operates with a 16Ω load for 2ms, drawing a current of 25 amperes. Between 2ms and 3ms, it operates with a 32Ω load, drawing a current of 12.5 amperes. Between 3ms and 4ms, it operates with a 48Ω load, drawing a current of 8.3 amperes. After 4ms, it operates with a 64Ω load, drawing a current of 6.25 amperes. Apart from the fluctuation during load changes, the output voltage is consistently maintained at 400V.

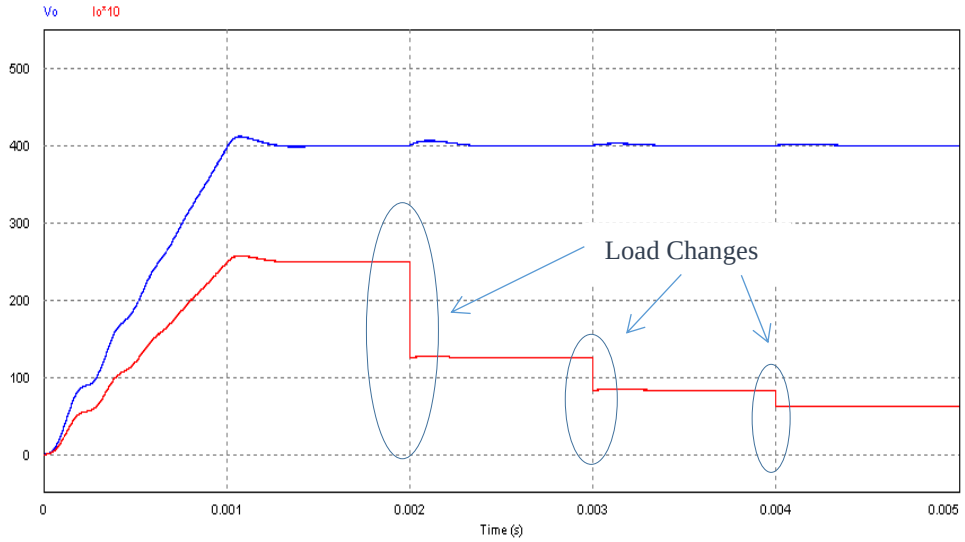

***Figure 4**. Output voltage and output current on variable load.*

The resonance current in the LCC resonant converter circuit is detected with the help of a sensor to control zero crossings, and switches S1 and S3 perform switching in zero current and zero voltage conditions. Switches S2 and S4, on the other hand, perform zero voltage switching by phase shifting according to the power state. As seen in Figure 5, when the output current Io is 25 amperes, the peak value of the current flowing through switch S1, denoted as Im, is around 70 amperes. However, since the switching is done at 110 kHz and in zero current, the switching losses are close to zero.

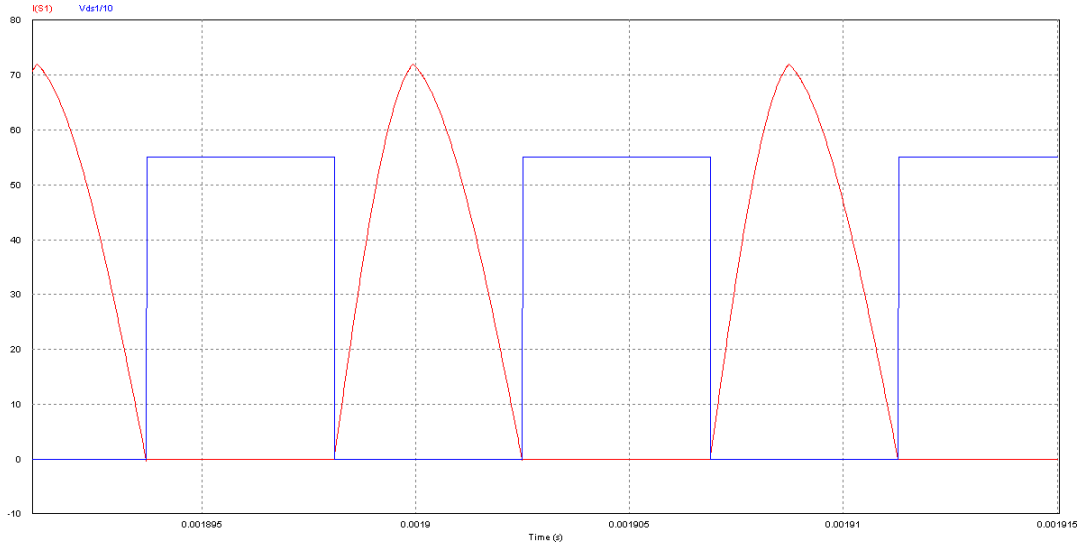

***Figure 5**. Current and voltage curves on the switching element (Io=25A, fs=110kHz).*

As seen in Figure 6, when the output current Io is 12.5A, the peak value of the current flowing through switch S1, denoted as Im, is around 53 amperes. Here again, since the switching is done at 120 kHz and in zero current, the switching losses are close to zero.

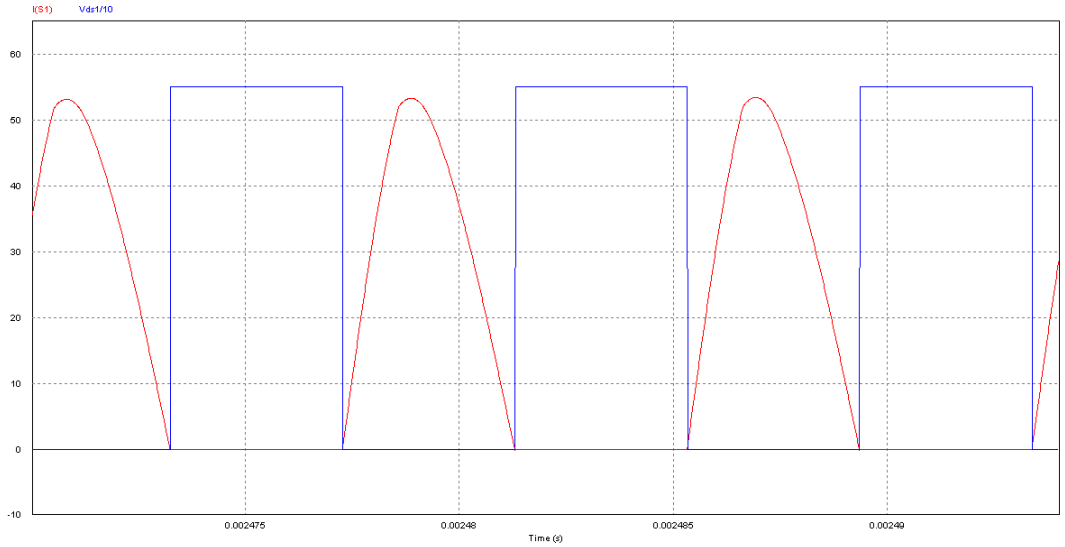

***Figure 6**. Current and voltage curves on the switching element (Io=12.5A, fs=120kHz).*

As seen in Figure 7, when the output current Io is 8.3 amperes, the peak value of the current flowing through switch S1, denoted as Im, is around 46 amperes. Similarly, here, since the switching is done at 127 kHz and in zero current, the switching losses are close to zero.

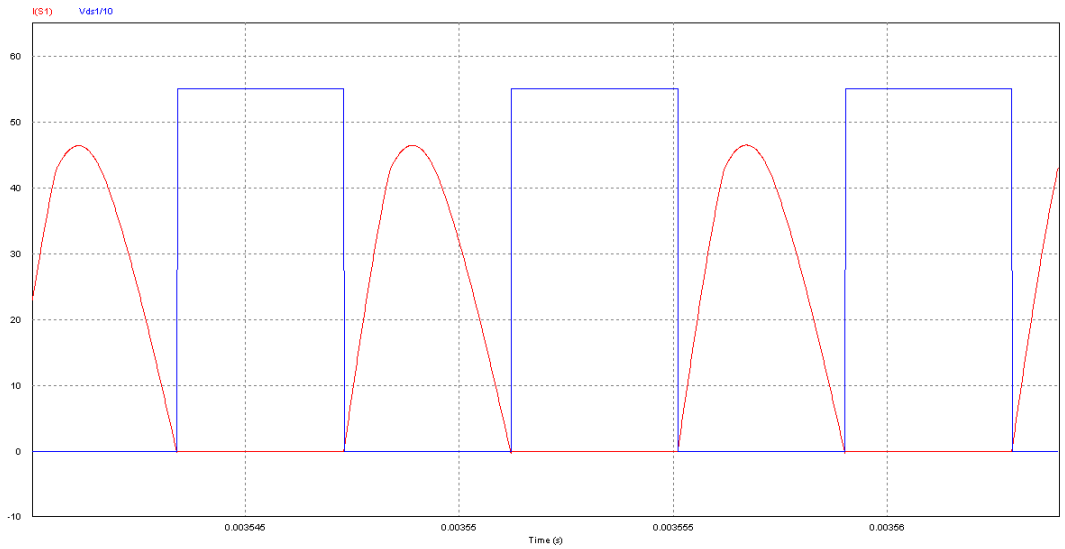

Figure 7*. Current and voltage curves on the switching element (Io=8.3A, fs=127 kHz).*

As shown in Figure 8, when the output current Io is 6.25 amperes, the peak value of the current flowing through switch S1, denoted as Im, is around 42 amperes. However, similarly, the switching is done at 130 kHz and in zero current, resulting in switching losses close to zero.

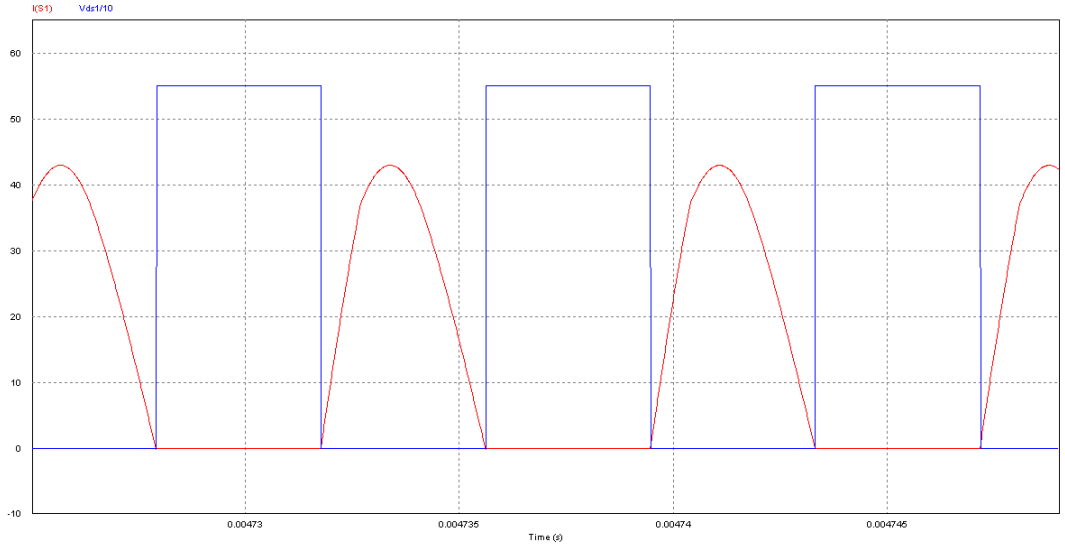

Figure 8*. Current and voltage curves on the switching element (Io=6.25A, fs=130 kHz).*

5. Conclusion

In this study, a straightforward algorithm has been devised to swiftly regulate the output voltage and switching frequency of the Full-Bridge Isolated LCC Series-Parallel Resonance circuit based on the current drawn by the changing load over time. The circuit is designed to operate with an input voltage of 550V, an output voltage of 400V, a maximum output current of 25A, and a variable operating frequency between 100-130kHz depending on the load condition. The algorithm detects the current flowing through the resonance circuit and the output voltage through sensors, ensuring the continuous resonance operation of the system and maintaining the output voltage at 400 volts even when the load changes. In converters employing PWM control, the switches operate under hard-switching conditions, leading to increased switching losses, current and voltage stresses on the switching elements, and electromagnetic interference (EMI) noise as the operating frequency rises. Achieving higher power density and faster transient response in DC-DC converters is only possible through an increase in the switching frequency. Therefore, it

has been demonstrated that reducing these losses and noises while simultaneously increasing the switching frequency can be achieved by implementing soft switching techniques. Simulation studies have presented the suitability of the series-parallel LCC-type circuit topology derived from resonant converter topologies, especially in scenarios involving variable loads such as batteries, and situations where a more stable output voltage is required.

REFERENCES

[1] Kazimierczuk, Marian K., and Dariusz Czarkowski. Resonant power converters. John Wiley & Sons, 2012.

[2] Oni, O. E., Davidson, I. E., & Mbangula, K. N. "A review of LCC-HVDC and VSC-HVDC technologies and applications", *16th International Conference on Environment and Electrical Engineering (EEEIC)* 1-7, 2016, doi: 10.1109/EEEIC.2016.7555677.

[3] Ahn, S. H., Jang, S. R., & Ryoo, H. J. "High-efficiency bidirectional three-phase LCC resonant converter with a wide load range", *IEEE Transactions on Power Electronics*, 34(1), 97-105, 2018, doi: 10.1109/TPEL.2018.2815078.

[4] Oncu, S., & Özbay, H. "Simulink model of parallel resonant inverter with DSP based PLL controller", *Elektronika ir Elektrotechnika*, 21(6), 2015, doi: 10.5755/j01.eee.21.6.13751.

[5] Yang, Rui, et al. "An Analytical Steady-State Model of LCC type Series–Parallel Resonant Converter With Capacitive Output Filter", *Power Electronics, IEEE Transactions on Power Electronics* 29(1), 328-338, 2014, doi: 10.1109/TPEL.2013.2248753.

[6] Arslan, L., & Özbay, H. "Modelling and simulation of D-class current-fed parallel resonant inverter for induction heating system", *Aintelia Science Notes*, vol. 1, no. 1, 106-116, 2022.

[7] Çayır, M., & Özbay, H. "PSIM simulation of voltage-fed series resonant inverter for induction heating systems", *Aintelia Science Notes*, vol. 1, no. 1, 117-126, 2022.

[8] Kang, H. W., Lee, H. S., Rhee, J. H., & Lee, K. A. "DC Voltage Source Based on a Battery of Supercapacitors with a Regulator in the Form of an Isolated Boost LCC Resonant Converter", *Energies*, 16(18), 6721, 2023, doi: doi.org/10.3390/en16186721.

[9] Feng, Y., & Kong, D. "Quasi-fixed frequency controlled phase modulation LCC resonant converter with a wide power range", *IET Circuits, Devices & Systems*, 17(3), 160-173, 2023), doi: 10.1049/cds2.12155.

[10] Lin, B. R. "Analysis of a Series-Parallel Resonant Converter for DC Microgrid Applications", *Processes*, 9(3), 542, 2021, doi: 10.3390/pr9030542.

[11] Sooksatra, S. "Analysis of asymmetrical LCC parallel resonant converter", *8th International Electrical Engineering Congress (iEECON)*, 1-4, 2020, doi: 10.1109/iEECON48109.2020.229526.

[12] Chen, J., Peng, H., Kang, Y., Wu, J., & Chu, X, "Accurate steady-state modeling and design based on state trajectory analysis for LCC resonant converter with voltage doubler rectifier", *IEEE Transactions on Power Electronics*, 37(9), 10698-10712, 2022, doi: 10.1109/TPEL.2022.3165591.

[13] Li, H., Xu, J., Gao, F., Zhang, Y., Yang, X., & Tang, H. "Duty cycle control strategy for dual-side LCC resonant converter in wireless power transfer systems", *IEEE Transactions on Transportation Electrification*, 8(2), 1944-1955, 2021, doi: 10.1109/TTE.2021.3123340.

[14] Song, Z., Gao, Y., & Shang, P. "Parameter design method of a series-parallel resonant converter". *4th Information Technology and Mechatronics Engineering Conference (ITOEC)*, 1024-1027, 2018.

[15] Jafari, H., & Habibi, M. "High-voltage charging power supply based on an LCC-type resonant converter operating at continuous conduction mode", *IEEE Transactions on Power Electronics*, 35(5), 5461-5478, 2019, doi: 10.1109/TPEL.2019.2946876.